Japan, the Society of Instrument and Control Engineers of Japan, and the Society of Automotive Engineers of Japan.

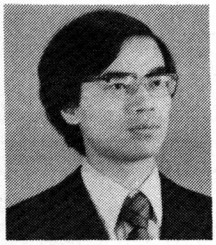

Haruo Naitoh was born in Imaichi, Japan, on June 17, 1952. He received the B.E. and M.E. degrees in engineering from the University of Tokyo, Tokyo, Japan, in 1975 and 1977, respectively.

He is currently a Postgraduate Student in doctoral courses at the University of Tokyo working on power electronics.

Mr. Naitoh is a member of the IEE of Japan.

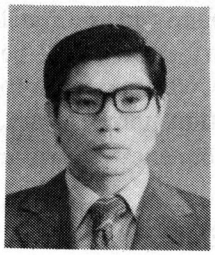

Toshimasa Haneyoshi was born in Tokyo, Japan, on January 28, 1949. He received the B.E. and M.E. degrees in engineering from Tokyo Denki University, Tokyo, Japan, in 1972 and 1975, respectively.

He was an Assistant Researcher at the Institute of Industrial Science, University of Tokyo, Tokyo, Japan, from 1975 to 1978. Since then, he has been an Assistant Researcher at Tokyo Denki University. During this time, he has been engaged in the study of power electronics. His interests also include nonlinear magnetic application.

Mr. Haneyoshi is a member of the IEE of Japan.

Losses and Parasitic Torques in Electric Motors Subjected to PWM Waveforms

FERNAND G. G. DE BUCK, MEMBER, IEEE

Abstract—**Some aspects of the theoretical performance of an electric motor, supplied by an unfiltered pulsewidth modulated (PWM) inverter are studied. The stator copper losses and the winding insulation lifetime are emphasized. An induction motor system is assumed and the creation of low-frequency parasitic torques are described. Their relative importance are estimated. It is shown that PWM supplies may have a negative impact on the motor performance and lifetime and can make a modification of the motor design more desirable than in the case where a "simpler" inverter system is used.**

NOMENCLATURE

RF	Resistance multiplication factor owing to skin effects.
v	$v = 1 \cdots M$, classification number for each set of conductors, starting at the bottom of the slot (Fig. 1).
M	Total number of conductor sets in a slot (Fig. 1).
PWM	Pulsewidth modulated.
F	Frequency.
R_{ac}, R_{dc}	ac and dc resistance ($R_{ac} = \text{RF} \cdot R_{dc}$).
Δ	Dimensionless conductor height ($\Delta = h/\delta$).
h	Height of one individual conductor layer (Fig. 1) composed of solid or paralleled conductors.
δ	Skin depth.
ρ	Specific resistance.
t	Temperature (°C).
n	Harmonic frequency number.
V_n, I_n	nth harmonic voltage and current.
sf, tf	Space fundamental, time fundamental.
sh, th	Space harmonic, time harmonic.
p	Number of pole pairs of the stator winding.
T	Torque.
$\cdots_S, \cdots_R$	Subscript ...stator, ...rotor.
d	Distortion.
N_S, N_R	Number of stator and rotor slots.
μ_0	$4\pi \cdot 10^{-7}$ H/m.
ω_{sy}	Synchronous rotational speed.
ω_R	Rotor rotational speed.
B	Magnetic field.
MMF	Magnetomotive force.

References for the per unit system are the nominal voltage, current, and motor impedance. Consequently, reference torque is larger than the nominal torque.

Paper ID 77-13, approved by the Industrial Drives Committee of the IEEE Industry Applications Society for presentation at the 1977 Industry Applications Society Annual Meeting, Los Angeles, CA, October 2-4.

The author is with the Laboratorium voor Nijverheidselectriciteit, State University, Gent, Belgium B.9000.

I. INTRODUCTION

A PULSEWIDTH modulated supply is often proposed and applied in the low-frequency region of a variable-frequency motor-drive system. Sometimes, the PWM operating region is extended towards and beyond the nominal 50 or 60 Hz motor frequency.

The PWM principle can eliminate all harmonics lower than the pulse harmonics, while higher ones (and especially the pulse harmonics) may increase considerably. Secondly, by means of a PWM inverter, the system structure and the transient performance of the motor can be improved, as the entire control action (voltage or current and frequency) concentrates on the single electronic part after the converter dc link and energy buffer. A filter at the ac output should be cheaper and smaller. For motor drives, such a filter is not always desirable, because during its operation, the motor requires a varying fundamental frequency and, as a result, a varying series of harmonic frequencies. Moreover, the filter may reduce the advantage of a PWM inverter concerning the control of the motor transient performance. Therefore, the first part of this paper, describing copper losses, assumes a direct machine-

0093-9994/79/0100-0047$00.75

inverter coupling, which is maintained around the nominal motor frequency. The theoretical motor performance will be analyzed and compared with its performance, when coupled to "simpler" inverter structures. The insulation temperature, copper losses, and the creation of low-frequency parasitic torques (a couple of hertz) are considered.

II. COPPER LOSSES AND WINDING TEMPERATURE

A. Calculation Model for the ac Losses and the Temperature Distribution

For many years, reliable formulas describing skin-effect losses in rectangular bars situated in open rectangular slots have been presented [1], [2]. In order to obtain a theoretical insight, this model will be adapted. According to Fig. 1, the formulas are

$$\mathrm{RF}(v, F) = R_{ac}(v, F)/R_{dc} \tag{1}$$

$$\mathrm{RF}(v, F) = \varphi(\Delta) + v(v-1)\Psi(\Delta) \tag{2}$$

with

$$\varphi(\Delta) = \Delta \frac{\sinh 2\Delta + \sin 2\Delta}{\cosh 2\Delta - \cos 2\Delta} \qquad \Psi(\Delta) = 2\Delta \frac{\sinh \Delta - \sin \Delta}{\cosh \Delta + \cos \Delta}$$

$$\Delta = h/\delta \qquad \delta = \left(\frac{B}{b} \cdot \frac{\rho}{\mu_0 \pi F}\right)^{1/2}.$$

In case of a nonsinusoidal supply, these expressions are easily extended. A complex waveform can be divided into a series of sinusoidal voltages and currents, and since no interaction between different frequencies occurs, all loss contributions can simply be added:

$$\mathrm{RF}(v) = \frac{\text{ac losses } (v)}{\text{dc losses } (v)} = \frac{\sum_n R_{ac}(v, n) I_n^2}{\frac{\rho(t(v))}{b \cdot h} I^2}$$

$$= \sum_n [\mathrm{RF}(v, t(v), n) \cdot (I_n/I)^2] \tag{3}$$

with

$$I^2 = \sum_n I_n^2.$$

Although no experimental results are available, these expressions can be assumed to be in reasonable accordance with reality, even for the deviating conductor and slot cross sections (e.g., semiclosed slots, circular conductors).

Special attention should be paid to the feedback action of temperature. Owing to higher losses and temperatures, the dc resistance increases, but the resistance factor RF is reduced due to a larger skin depth. Eventually, these opposite actions might lead towards a limitation of the losses and the temperature rise. It turns out, however, that this effect is of low importance and is not capable of keeping the winding temperature within reasonable limits.

Starting from the winding losses, the temperature distribution is calculated, using the heat-flow expressions:

$$\left(1.5 + \frac{2.5}{M}\right) t(M) - t(M-1) = \mathrm{RF}(M) \frac{3.5(100 - t_{iron})}{M} + \left(0.5 + \frac{2.5}{M}\right) t_{iron} \tag{4}$$

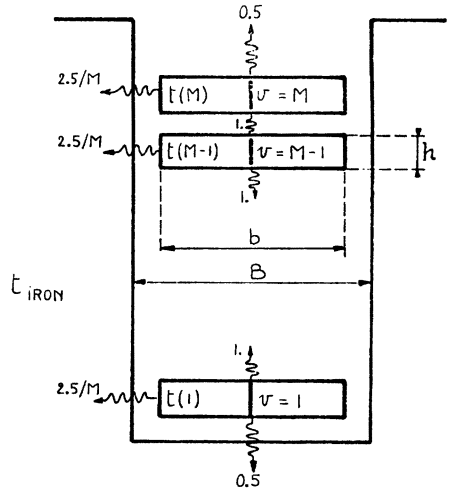

Fig. 1. Cross section of slot and its embedded conductors; heat-flow model.

$$-t(v+1) + \left(2 + \frac{2.5}{M}\right) t(v) - t(v-1) = \mathrm{RF}(v) \frac{3.5(100 - t_{iron})}{M} + \frac{2.5}{M} t_{iron} \qquad [v = 2 \cdots M-1] \tag{5}$$

$$-t(2) + \left(1.5 + \frac{2.5}{M}\right) t(1) = \mathrm{RF}(1) \frac{3.5(100 - t_{iron})}{M} + \left(0.5 + \frac{2.5}{M}\right) t_{iron}. \tag{6}$$

These expressions are easily obtained by relating the heat production to the thermal insulation coefficients and the resulting temperature differences (Fig. 1). It is assumed that the average winding dc temperature and the iron temperature are equal to 100°C and 60°C, respectively. The relative heat transfer coefficients towards the four boundaries have been logically chosen and indicated in Fig. 1.

The impact of the winding temperature on the specific resistance, and thus on the skin depth, can be described by

$$\rho = 230\ 10^{-10}(1 + 0.0028(t - 100))\Omega m. \tag{7}$$

This equation can be used for copper windings at a temperature situated between 100-200°C. Within the calculation process, the temperature feedback action is responsible for the creation of an iteration cycle.

B. Selection of Representative PWM Supplies

In order to compare the performance of a PWM-fed motor with its performance when coupled to a sinusoidal or square wave voltage supply, some representative waveforms have been picked out. Two PWM waves with a relatively high pulse number are chosen. Their shape is constructed using the intersection points of a sinusoidal and a triangular wave with a respective relative height of 1 and 1.25. The Fourier components of the voltage waves are listed in Table I. Neglecting all third harmonics and assuming an induction motor leakage or synchronous motor subtransient reactance of approximately 0.2 per unit, the corresponding harmonic currents are calculated and indicated as well.

TABLE I
FREQUENCY COMPONENTS OF VOLTAGE AND CURRENT FOR SOME PWM WAVEFORMS AND FOR SQUARE WAVE VOLTAGE SUPPLY

n	PWM_{12} 12 pulses per cycle		PWM_{24} 24 pulses per cycle		SWV square wave voltage		sinusoidal supply	
	V_n	I_n	V_n	I_n	V_n	I_n	V_n	I_n
1	1.	1.	1.	1.	1.	1.	1.	1.
5	0.	0.	0.	0.	0.2	0.2		
7	0.	0.	0.	0.	0.14	0.102		
11	0.4	0.179	0.	0.	0.09	0.041		
13	0.4	0.154	0.	0.	0.077	0.03		
17	0.04	0.012	0.	0.	0.059	0.017		
19	0.11	0.029	0.	0.	0.053	0.014		
23	0.13	0.028	0.4	0.087	0.043	0.01		
25	0.13	0.026	0.4	0.08	0.04	0.008		
29	0.18	0.031	0.	0.	0.035	0.006		
31	0.09	0.015	0.	0.	0.032	0.005		
d	0.64	0.24	0.57	0.12	0.29	0.23	$d=\left[\sum_{n>1}(V_n \text{ or } I_n)^2\right]^{1/2}$	

All third harmonics are neglected; leakage reactance is equal to 0.2 per unit.

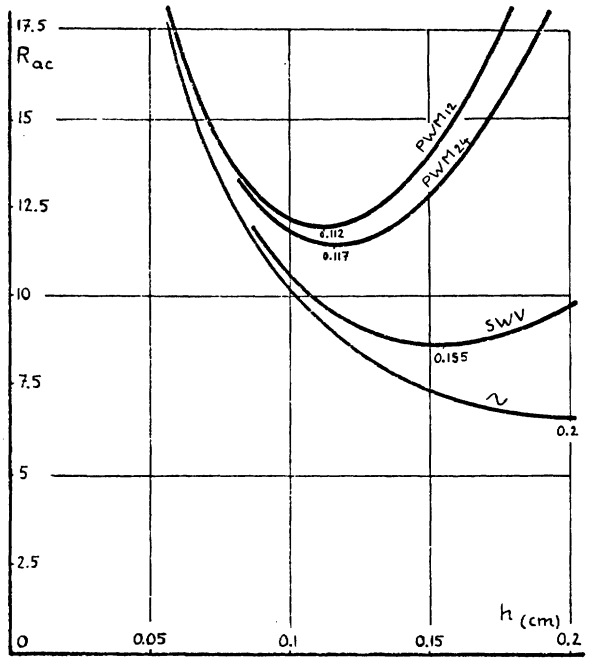

Fig. 2. Average ac resistance in function of conductor height ($M = 50$; $F_1 = 50$ Hz); no temperature feedback.

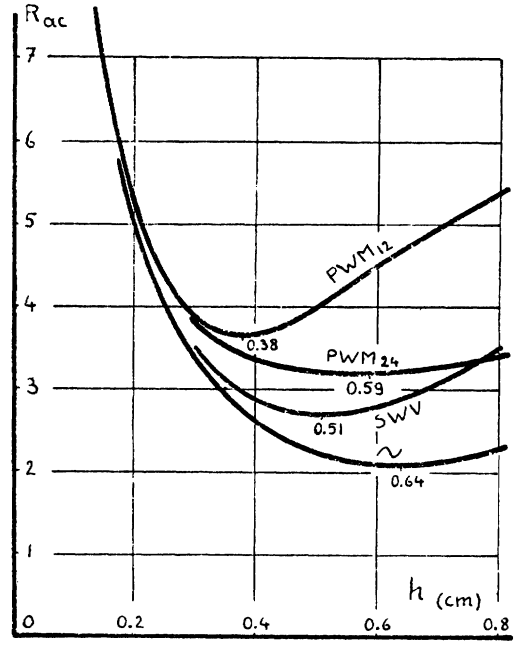

Fig. 3. Average ac resistance in function of conductor height ($M = 50$; $F_1 = 50$ Hz); no temperature feedback.

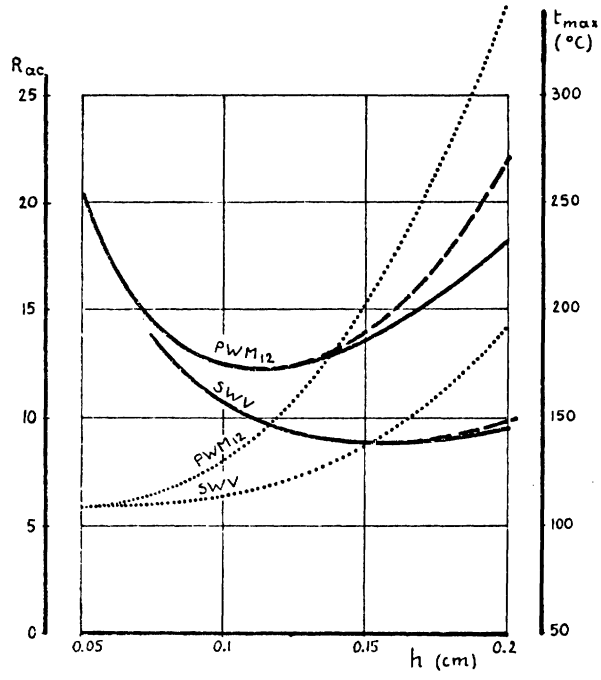

Fig. 4. Influence of winding temperature on average ac resistance ($M = 50$). --- ac-resistance; no temperature feedback. — ac-resistance; temperature feedback included. ··· maximal winding temperature; temperature feedback included.

C. Stator Copper Losses–Results

All results are calculated using (1) to (7) for b/B equal to one and assuming a fundamental frequency of 50 Hz. As the number of conductor layers can be selected within a broad range, M was chosen equal to 5 and 50.

Figs. 2 and 3 represent the course of the average ac resistance for a varying conductor height h. M is constant and equal to 50 and 5, respectively. Temperature feedback is neglected.

Fig. 4 analyzes the impact of the temperature on the ac resistance. The maximum winding temperature has been indicated as well. It is clear that the influence of the temperature becomes important only if the conductor height is sufficiently larger than the critical height for minimal resistance. The winding temperature is not restrained by this feedback action, but is increasing towards a level, such that the insulation is degraded very rapidly.

Figs. 5 and 6 represent the distribution of the temperature, losses, and resistance factor over the slot windings, respectively, for M equal to 5 and 50. These figures correspond to the critical conductor height for which the average ac resistance is minimal. Although they actually correspond to a PWM_{12} supply, they are quite independent of the supply nature, as long as the height h keeps critical.

These and similar figures lead toward Tables II and III, which provide the critical conductor heights (centimeters) and

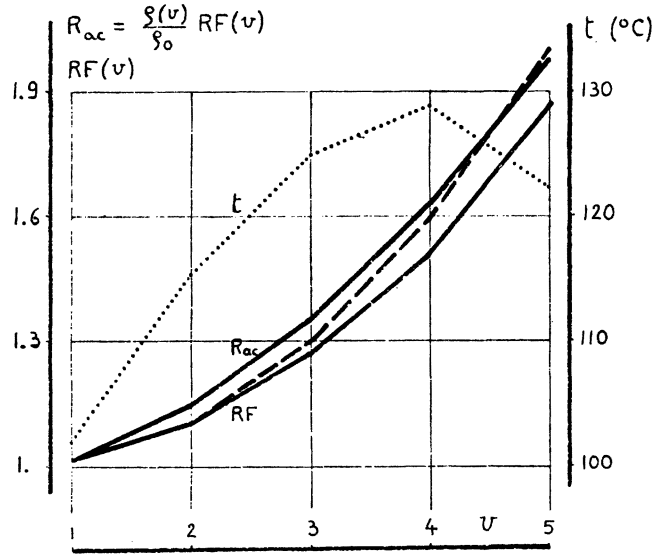

Fig. 5. Distribution of temperature, losses, and resistance factor over slot windings (M = 5; PWM_{12}), assuming that conductor height is critical (h = 0.38 cm). --- R_{ac} and RF; neglecting temperature feedback. — R_{ac} and RF; temperature feedback included. ··· winding temperature.

TABLE II
CRITICAL VALUES FOR CONDUCTOR HEIGHT, AVERAGE RESISTANCE, AND RESISTANCE FACTORS

supply waveform	$h_{critical}$ (cm)	$R_{minimal}$	$RF_{average}$	$RF_{v=M}$
sinusoidal	0.2	6.6	1.33	1.98
SWV	0.155	8.6	1.34	2.01
PWM_{12}	0.112	11.9	1.34	1.99
PWM_{24}	0.117	11.4	1.34	2.0

For different supply waveforms and for M = 50 (no temperature feedback).

TABLE III

supply waveform	$h_{critical}$ (cm)	$R_{minimal}$	$RF_{average}$	$RF_{v=M}$
sinusoidal	0.64	2.1	1.33	1.86
SWV	0.51	2.6	1.38	1.94
PWM_{12}	0.38	3.6	1.42	2.03
PWM_{24}	0.59	3.2	1.90	3.21

See table II; M equal to 5.

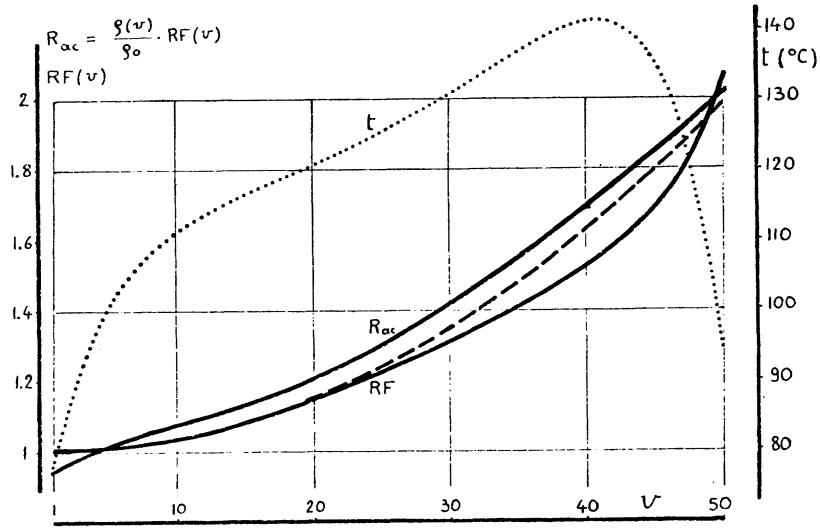

Fig. 6. Distribution of temperature, losses, and resistance factor over slot windings (M = 50; PWM_{12}), assuming that conductor height is critical (h = 0.112 cm). --- R_{ac} and RF; neglecting temperature feedback. — R_{ac} and RF; with temperature feedback. ··· winding temperature.

the corresponding minimal average ac-resistance values (R is equal to one for a conductor with a height of 1 cm). The average resistance factors and the factors corresponding to the top conductors are also indicated. As these values are not substantially influenced, no temperature feedback has been taken into account.

D. Discussion

Although the current distortion levels of the investigated PWM waveforms are comparable or smaller than those for a square wave voltage supply (Table I), the slot copper losses may increase by more than 50 percent (Figs. 2-4). At the same time, the corresponding critical conductor heights are reduced with some 30 percent (Tables II and III). A larger PWM pulse number does not tend to improve this situation substantially. These conclusions especially yield for slot windings with many conductors; windings with a low M give a somewhat less stringent situation. It should be emphasized that for a PWM_{24} supply (M = 5, Fig. 3) the minimal resistance cannot be reached, due to a too high winding temperature (Table III: $RF_{v=M}$ = 3.21).

In case the conductor height is critical, Figs. 5 and 6 show that the maximum winding temperature can increase with some 20-35°C. Consequently, if such motors have a low insulation quality, they may experience an important lifetime reduction of, for example, more than 70 percent, in comparison with the lifetime under sinusoidal supply. The application of a higher grade insulation becomes compulsory. Exceeding the critical height results in a sharp rise of the temperature (Fig. 4). As emphasized in the introduction, these conclusions are only

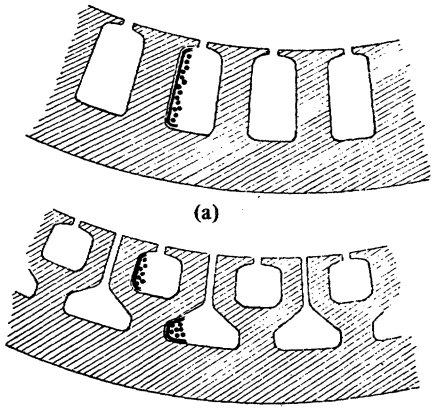

Fig. 7. (a) Conventional stator slot punching. (b) Modified punching with increased slot number and reduced slot depth.

important if the unfiltered PWM supply is used at or around the nominal motor frequency.

For critical dimensions, the average and maximal resistance factors and losses are mostly equal to 1.3 ··· 1.4 and 1.8 ··· 2, respectively. These values are quite independent of the waveform (Tables II and III). Exceptions do occur (PWM_{24}, Fig. 3, Table III).

E. Motor Design Indications

As pointed out, an improvement of the insulation quality and of the heat transport to the slot boundaries may be necessary. However, this measure has no influence on the actual losses. An artificial increase of the motor leakage reactance seems likely, as the harmonic currents are inversely proportional to the leakage and as the contribution to the losses is proportional to the square of the current. This measure, easy to accomplish, can be sufficient if the maximum fundamental frequency at full motor current is limited to about 50 or 60 Hz and if the harmonic content is not too high. It may not be sufficient for PWM supplies. The induction-motor leakage must be restricted to about 0.4 per unit or even considerably lower [6], mainly depending on the required per unit steady-state pull-out torque. In contrary, the steady-state maximum torque of a synchronous motor is less leakage-dependent. An increase of the leakage reactance may have undesirable effects on the system transient response due to a larger time constant.

In case a higher leakage should be insufficient or not desirable owing to steady-state or transient requirements, a modification of the winding design or the slot punching should be considered. The application of narrower parallel connected and transposed Litz wire-type windings, and/or a wider but shallower slot cross section may be regarded. Eventually, as this last measure is quite restricted, the slot punching can be modified into a set of two rows of shallow slots situated one above the other (Figs. 7(a) and (b)). Due to a larger slot number and a reduction of the slot current, this measure does not necessarily lead towards an increase of the leakage reactance.

Analogous to the negative sequence limit of synchronous generators, an existing motor design should be characterized by some maximum tolerable voltage distortion. Due to the wide spread in distortion nature (e.g., SWV or PWM_{12}), such a coefficient will be difficult to determine.

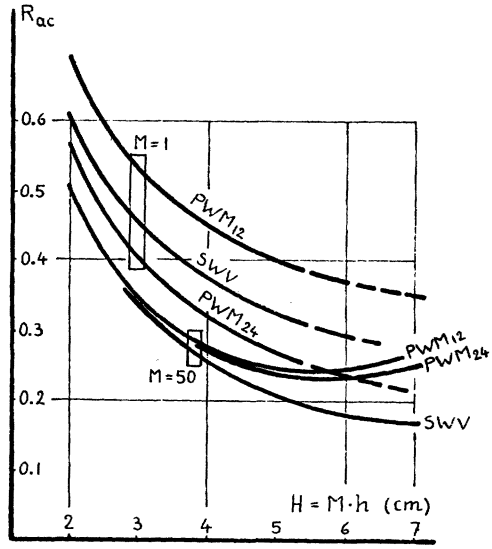

Fig. 8. Rotor bar ac resistance in function of total available conductor height; $M = 1$ and $M = 50$.

F. Remarks Concerning Induction-Motor Rotor-Cage Losses (Fig. 8)

Cage losses can be calculated in a similar way, taking into account that M equals one and that all frequencies have to be adapted. Because $M = 1$, an increase of the pulse number becomes advantageous, and the losses caused by a PWM_{24} supply are situated well below those for a square wave voltage (Fig. 8). Although the harmonic-induced losses are higher than in the case when the cage is replaced by a closed-coil structure, the allowed temperature increase is not restricted in the same severe way; as the rotor bars are rarely insulated, insulation lifetime requirements do not exist.

III. LOW-FREQUENCY PARASITIC TORQUES IN INDUCTION MOTORS

As many inverter-fed induction motors will operate continuously within the narrow-slip range around synchronous speed, the distortion of the high-slip acceleration characteristic by parasitic torques is not important. Within the low-slip region, a nonsinusoidal supply will always create some high-frequency oscillating torques. This phenomenon has often been described and is not taken into account in this paper.

Under some conditions, high-amplitude pulse harmonics can create parasitic synchronous and low-frequency pulsating torques (a couple of Hertz), even when the motor is running at about its nominal speed (50 or 60 Hz). As a consequence, some resonance phenomena can appear within a wide speed range [4]. This requires that the stator or rotor slot number per pole-pair is more or less equal to the supply pulse number or to the dominating supply harmonics. The relative importance can be predicted and estimated by decomposition of the airgap field into a set of sinusoidally distributed MMF and permeance fields in analogy with Alger's MMF and permeance method [5]. Each time-harmonic frequency of the supply waveform is

now responsible for such a complete set of space-harmonic fields. Many torque interactions occur, only some of which are important. The most important interactions, causing a low-frequency pulsating torque, will be selected and estimated.

1) A time-harmonic stator current creates space-harmonic rotating stator fields, which, on their turn, cause rotor currents in the cage of an induction motor. The most important of these stator fields are the slot MMF and permeance harmonics. The induced rotor currents corresponding to these latter fields create a series of sh rotor fields with a pole-pair number

$$p' = N_S \pm N_R \pm p \tag{8}$$

and with a rotational speed, refering to the stator frame, which is represented by (see appendix):

$$\frac{\omega'}{p} = \left(\frac{n_{\mathrm{PWM}}\omega_{\mathrm{sy}}}{N_S \pm p} - \frac{\omega_R}{p}\right)\frac{N_S \pm p}{N_S \pm N_R \pm p} + \frac{\omega_R}{p}. \tag{9}$$

Depending on the choice of the two slot numbers, one of these latter fields may have p pole-pairs and thus interacts with the dominating tf-sf stator field. This occurs if $p' = \pm p$. The interaction will have a LF nature within a narrow motor slip range which depends on the ratio of the slot numbers to the dominant time-harmonics in the supply waveform. A creation of LF parasitic torques during normal motor operation, in the way as described, requires that

$$p' = \pm p$$

$$\omega'/p = \omega_{\mathrm{sy}}/p, \qquad \text{for } \omega_R/p \approx \omega_{\mathrm{sy}}/p.$$

As a result, the simultaneous fulfillment of the following conditions is required (using (8) and (9)):

a) the motor must have a cage type rotor;
b) $N_S = N_R \pm 2p$ or $N_S = N_R$;
c) $n_{\mathrm{PWM}} \approx N_S/p \pm 1$.

Assuming nonskewed rotor slots, the amplitudes of the LF torques can be approximated, using (see appendix):

$$\frac{T_{\mathrm{parasitic}}}{T_{\mathrm{nominal}}} \approx (1 \cdots 2) \cdot \left[\frac{1}{(N_S/p)}\frac{I_{S,n}}{I_{S,1}} + \frac{1}{4n_{\mathrm{PWM}}}\frac{V_n}{V_1}\right] \cdot \left[\frac{N_R}{p}\left(\frac{\sin N_S\pi/N_R}{N_S\pi/N_R}\right)^2\right]. \tag{10}$$

The second factor on the right side of (10) estimates the amplitude of, respectively, a MMF and a permeance th-sh stator wave. The last factor estimates the induced th-sh rotor current and that particular resulting rotor field which has p pole-pairs. Very small motors or motors with many poles ($N_S/p = 6$), supplied by a PWM inverter with a low pulse number ($n_{\mathrm{PWM}} \approx 6$; $V_n/V_1 \approx 0.6$; $I_{S,n}/I_{S,1} \approx 0.6$) can produce LF torques which attain 2-20 percent of the nominal torque. For larger motors, with $N_S/p \geq 12$, supplied by a PWM inverter with at least 12 pulses per cycle ($V_n/V_1 \approx 0.4$; $I_{S,n}/I_{S,1} \approx 0.15$), this number is smaller than 2 percent.

2) Synchronous and LF torques can be produced by superposition of permeance and MMF harmonics. The product of two such waves can form a resulting field component with a fundamental pole-pair number p. The induced rotor currents with space-fundamental pole-pair number can interact with the space-fundamental field wave of another time-harmonic supply component and thus create LF parasitic torques. Such interaction may now occur, for cage motors as well as for slip-ring motors. The fulfillment of a condition concerning the rotor slot number is required. The following conditions are obtained:

a) squirrel-cage or slip-ring motor,
b) $N_S = N_R \pm 2p$ or $N_S = N_R$,
c) $n_{\mathrm{PWM}} \approx N_R/p \pm 1$.

These conditions are obtained in a way, similar as used in 1). The amplitude can be roughly estimated using

$$\frac{T_{\mathrm{parasitic}}}{T_{\mathrm{nominal}}} \approx (1 \cdots 2) \cdot \left[\frac{0.25V_n}{8n_{\mathrm{PWM}}V_1} + \frac{0.5I_{S,n}}{2(N_S/p)I_{S,1}}\right]. \tag{11}$$

The first term results from the superposition of a stator permeance and a rotor permeance wave with a space-fundamental wave. The second term results from the superposition of, for example, a rotor permeance wave with a stator MMF wave.

A motor with $N_S = 6p$, fed by a six-pulse inverter, may give a result situated between 1-5 percent. Larger motors yield a torque smaller than 1 percent.

As a result, only very small motors, supplied by a low-pulse inverter, may produce LF oscillating torques of considerable amplitude. In case of squirrel-cage motors, such torques occur only if the rotor slot number is chosen in an uncommon way. If the rotor slots are skewed, a further torque reduction will be obtained. In addition to the possibilities described in this section, many other less important LF torques can be created.

IV. CONCLUSIONS

This paper has called attention to two particular aspects of the motor performance, which may be of importance within a restricted number of applications.

1) PWM-induced copper losses can increase with even more than 50 percent depending on the winding design, the fundamental frequency, and the degree of filtering. The losses are mostly situated well above those corresponding with a square wave supply. The critical conductor height, corresponding with the minimal ac resistance, can be exceeded more quickly, involving a high and unequally distributed winding temperature and thus reducing the expected motor lifetime. Some design modifications have been provided. A reduction of the harmonic content by increasing the pulse number does not necessarily offer a substantial improvement. The application of a PWM inverter within a broad time-fundamental frequency range thus offers disadvantages, unless it is possible and intended to filter the output.

2) Besides HF torques, small motors or motors with a high pole-pair number may experience low-frequency torques within a broad speed range. The most important origins have been described and estimated. Such torques may occur if one of the induction-motor slot numbers is approximately equal to the pulse number. These torques will rarely be important.

As a conclusion, within the particular range of motor-inverter applications described in this paper, a PWM power-electronic system with possibly higher complexity does not necessarily create better motor performance. In contrary, it can make modification of the motor design more necessary than in the case where a "simpler" square wave inverter is used.

APPENDIX

Equation 9 is derived knowing that the MMF or permeance space-harmonic stator field with $N_S \pm p$ pole-pairs, created by a time-harmonic current, revolves with an angular velocity

$$\omega_a/p = n_{\mathrm{PWM}}\omega_{\mathrm{sy}}/(p \pm N_S)$$

related to the stator frame, or

$$\omega_b/p = \omega_a/p - \omega_R/p$$

related to the rotor frame. The corresponding induced rotor currents create sh rotor fields. For our discussion, the most important fields have a pole-pair number

$$p' = N_S \pm p \pm N_R \tag{8}$$

and an angular velocity, related to the rotor frame

$$\omega_c/p = (\omega_b/p)\frac{N_S \pm p}{N_S \pm N_R \pm p}$$

or related to the stator frame

$$\omega'/p = \omega_c/p + \omega_R/p. \tag{9}$$

As a first approximation, (10) is obtained knowing that

$$\frac{T_{\mathrm{parasitic}}}{T_{\mathrm{nominal}}} \approx \frac{B_{R,\mathrm{thsf}}}{B_{R,\mathrm{tfsf}}} \approx \frac{B_{R,\mathrm{thsf}}}{B_{S,\mathrm{thMMF\ and\ permeance}}} \cdot \frac{B_{S,\mathrm{thMMF\ and\ permeance}}}{B_{S,\mathrm{tfsf}}} \cdot \frac{B_{S,\mathrm{tfsf}}}{B_{R,\mathrm{tfsf}}} = C_1 \cdot C_2 \cdot C_3$$

with

$$C_3 \gtrapprox 1$$

$$C_2 \approx \frac{B_{S,\mathrm{thMMF}}}{B_{S,\mathrm{tfsf}}} + \frac{B_{S,\mathrm{th\ permeance}}}{B_{S,\mathrm{tfsf}}} \approx (p/N_S) \cdot \frac{I_{S,n}}{I_{S,1}} + \frac{1}{4n}\frac{V_n}{V_1}.$$

C_1 takes account of the consideration that the largest part of the stator space-harmonic field functions as a leakage field. As a result, the induced rotor currents are small. According to [2], C_1 can be estimated:

$$C_1 \approx \frac{N_R}{p}\left[\frac{\sin(\pi N_S/N_R)}{\pi N_S/N_R}\right]^2.$$

Equation 11 is derived in a similar way.

REFERENCES

[1] R. Richter, *Elektrische Maschinen*; Band 1: *Allgemeine Berechnungselemente*; *Die Gleichstrommaschinen*, 3rd Ed., Birkhäuser Verlag, Basel 1967, Ch. L, pp. 237–264.

[2] R. Richter, *Elektrische Maschinen*; Band 4: *Die Induktionsmaschinen*, 2nd Ed., Birkhauser Verlag, Basel 1954, Ch. F, pp. 119–131, Ch. H, pp. 176–217.

[3] H. C. J. de Jong, *AC motor design with conventional and converter supplies.* Oxford, England: Oxford Univ., 1976, Ch. 6, 7, pp. 68–83.

[4] P. N. Bapat, "Frequency response of induction motors under forced oscillations," *Proc. IEE*, vol. 117, no. 3, pp. 561–566, Mar. 1970.

[5] P. L. Alger, *Induction Machines,* 2nd Ed. New York: Gordon and Breach, 1970.

[6] F. G. G. De Buck, "Design adaptation of inverter-supplied induction motors," *IEE Electric Power Applications*, vol. 1, no. 3, pp. 54–60, May 1978.

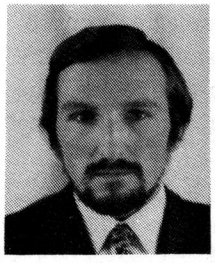

Fernand G. G. De Buck (S'75–M'77) was born in Gent, Belgium, on February 21, 1952. He received the electrical and mechanical engineering degrees from the State University, Gent, in 1974, and the M.S.E.E. degree from the Massachusetts Institute of Technology, Cambridge, in 1976. He is currently working towards a Ph.D. degree, conducting research on the design of inverter-supplied electric motors, under financial assistance of the Belgian National Foundation for Scientific Research.